PCCP

# Theory and simulation of biaxial nematic and orthogonal smectic phases formed by mixtures of board-like molecules

**A. G. Vanakaras,[a] M. A. Bates*[ab] and D. J. Photinos[a]**

[a] *Department of Materials Science, University of Patras, Patras 26500, Greece*
[b] *Department of Chemistry, University of Southampton, Southampton, UK SO17 1BJ.*
*E-mail: bates@soton.ac.uk*

***Received 3rd June 2003, Accepted 4th July 2003***
***First published as an Advance Article on the web 24th July 2003***

Variational cluster calculations and Monte Carlo simulations are applied to hard-body board-like models of biaxial molecules forming liquid crystalline phases. The molecular long axes are assumed for simplicity to be fully oriented. Depending on the extent of transverse anisometry in the molecular shape, these systems can exhibit biaxial nematic phases as well as uniaxial and biaxial orthogonal smectic phases. It is shown that the region of thermodynamic stability for the biaxial nematic phase is considerably broadened in binary mixtures of molecules with the same cross section but differing in their long dimension.

## I. Introduction

The existence of thermotropic biaxial nematics is one of the long standing problems in liquid crystal science. They have been constantly attracting experimental, theoretical and computer simulation research interest for over three decades[1–44] and yet no stable low molar mass thermotropic biaxial nematic phase has to date been conclusively identified by experiment. In fact, reports on the observation of any type of real biaxial nematic phase, be it in a lyotropic[5] or polymeric[19] system, are scarce in the literature. Indeed, there are several instances of systems that were initially reported as biaxial nematics but these were later found not to be so.[28,38] However, preliminary reports provide strong indications that thermotropic biaxial phases may have been stabilised in at least two different cases, namely bent-core mesogens[45] and rod-plate systems.[46] Indeed, an orthogonal biaxial smectic phase has already been reported for banana shaped molecules.[47,48]

On the other hand, theory and computer simulations not only support the possibility of thermodynamically stable biaxial nematic phases but also suggest several molecular models and corresponding approaches for the realization of biaxial nematics .[1–4,6–18,20–27,29–37,39–43] However, of equal importance to supporting the possibility of biaxial nematic phases, theoretical and computer simulation investigations also give a useful insight into why the realization of such systems is difficult .[12–14,30,35,40] Thus, for example, the seemingly simple approach of generating a biaxial nematic phase by mixing two uniaxial phases with non-coincident directors, typically a rod-nematic and a disc-nematic phase, is plagued by difficulties with the miscibility of the components[12,13,21,26,40,42,43] and, as model calculations suggest, some chemically demanding fine tuning of the molecular associations is required in order to keep the constituent phases together as a biaxial fluid rather than phase separating into the two uniaxial phases.[30,35,40]

Stabilization of biaxial phases in single component systems is based on the optimisation of the molecular (typically shape) biaxiality. These approaches are faced with difficulties of a different kind. Molecular biaxiality, although readily quantifiable in the context of various models and idealized representations of molecules, becomes difficult to quantify in the case of actual thermotropic nematic molecules (nematogens), where different types of interactions are present that cannot be ignored. This renders the transcription of the 'optimal' molecular biaxiality into a concrete chemical structure a major task in itself. This task is further complicated by molecular flexibility, which is not negligible for common nematogens at finite temperatures, and makes it necessary to consider simultaneously many conformations for the evaluation of the 'average' biaxiality. The major difficulty associated with the latter is that the average biaxiality could differ considerably between isolated molecules and molecules in the nematic bulk where, for example, low energy conformations could become disfavoured due to their inefficient packing relative to other, higher energy conformations that pack more efficiently.[35] Finally, what is required of the 'optimal' molecular biaxiality is not only to stabilise the biaxial nematic phase relative to the uniaxial nematic but relative to all the other possible competing phases, such as the smectic and the columnar fluid phases and the solid phases. Given the aforementioned difficulties, a systematic determination of actual molecular structures that satisfy all the requirements for nematic biaxiality is a rather complex matter.

Part of the complexity can in principle be removed if the stabilization of the biaxial nematic relative to its non-nematic competitors can be enhanced independently of the optimisation of molecular biaxiality. What is essentially sought in this case is a mechanism to destabilise the competing phases without affecting the stability of the biaxial nematic relative to the uniaxial nematic phase. The present work concerns the exploration of such mechanism for rod-like or prolate biaxial nematogens. In this case the prime competing phases are the layered smectic phases, which may be uniaxial or biaxial.

We examine the possibility of extending the biaxial nematic range by destabilizing the smectic phase that occurs at higher densities or lower temperatures. Simulation studies of uniaxial systems of two-component mixtures of parallel spherocylinders of differing length and long spherocylinders with polydispersity in length[49,50] have shown that the smectic phase can be destabilized since the layered structure cannot accommodate the differing lengths. In these studies of uniaxial particles with a circular cross section, the smectic phase is often replaced with a columnar phase and so the nematic range is not extended

DOI: 10.1039/b306271f

significantly. However, if the particles are not uniaxial then the columnar phase should be less favoured, since they would not be expected to pack efficiently into columns without first aligning to form an ordered, biaxial phase. The use of mixtures of biaxial particles of differing lengths should, therefore, allow us the possiblility of extending the range of the biaxial nematic phase for systems in which it exists, or reveal a biaxial nematic phase in systems that would form this phase, if the smectic phase was not present. Essential to this alternative approach towards stable biaxial nematics is that the two (or more) components of the mixture do not generate miscibility difficulties. This could be achieved by using molecules of different lengths but of identical transverse cross section.

In this paper we use variational cluster expansion theory, in the two-site cluster approximation,[51] and Monte Carlo computer simulations to investigate these ideas. To model the biaxial molecules we use a simple hard body idealisation of the molecular shape, namely a lath shaped cuboid of dimensions $a$:$b$:$c$ (with $a \gg b > c$). In the limit that one dimension of the particles is much larger than the other two, we only need to consider the limiting case of perfectly aligned system. This is because we expect that the (uniaxial) nematic–isotropic transition will occur at much lower densities than any transition from a uniaxial nematic to either a biaxial nematic or a uniaxial or biaxial smectic. The former will be similar to the nematic–isotropic transition exhibited by infinitely long uniaxial rods[52] and so will occur at vanishingly small densities. Within this approximation, we limit ourselves to a simple model for studying systems of long biaxial particles which possess a uniaxial nematic phase. Clearly, this model cannot be used to investigate the critical point in the phase diagram where the continuous isotropic to biaxial nematic (I–$N_{BX}$) transition is predicted to occur as the behaviour shifts from that of a rod-like particle (I–$N^+$–$N_{BX}$) to that of a disk-like one (I–$N^-$–$N_{BX}$). This has been studied elsewhere both theoretically[4] and by simulation.[18] A particular advantage of studying perfectly ordered systems, is that the length of the particle need not be specified because an affine transformation along the director will not change the properties of the system, apart from a trivial scaling of the density and pressure. Since the length need not be specified, we characterize the shape biaxiality of the particles $r$ by the ratio of the other two dimensions, namely $r = b/c$. The above simplifications lead to a highly idealised representation of the common thermotropic liquid crystalline phases. Such a description is, however, adequate for the presentation of the basic idea, namely destabilising the smectic phases to reveal or extend the biaxial nematic phase.

The rest of the paper is laid out as follows. In Section II, we describe how the phase stability and hence the phase diagrams may be obtained by theoretical methods. We use computer simulations of the same models, which are also described in Section II, to test the theoretical predictions. The phase diagram for a single component system of aligned biaxial laths as a function of their biaxiality is presented in Section III. In Section IV we consider how this phase diagram changes when mixtures of particles with differing lengths are used. Finally, we discuss results and present our conclusions in Section V.

## II. Variational cluster theory and computer simulations

The aim of the theoretical calculations is to determine the liquid crystal phase behavior of a binary mixture composed of lath-like particles with their molecular $z$-axes perfectly oriented parallel to the macroscopic $Z$-axis. The translations of the molecules as well as rotations about their $z$-axis are unrestricted. Under these conditions, the least ordered phase of the system is a homogeneous phase with uniformly distributed molecular rotations about the $z$-axis. This implies for the principal order parameters $\langle \cos 2\varphi \rangle = \langle \cos 4\varphi \rangle = 0$, where the angle $\varphi$ describes rotations about the molecular $z$-axis and the angular brackets denote equilibrium ensemble averages. This phase is described as uniaxial nematic, $N_U$, and the macroscopic $Z$-axis is a $C_\infty$ axis. The system can exhibit two more uniform phases but of higher orientational order, consistent with the molecular symmetries:

The first phase is described as tetratic nematic, $N_T$, wherein the macroscopic $Z$-axis is a $C_4$-axis. Here $\langle \cos 2\varphi \rangle = 0$ and $\langle \cos 4\varphi \rangle \neq 0$.

The second is described as biaxial nematic phase, $N_{BX}$, and the macroscopic $Z$-axis is a $C_2$-axis. Here $\langle \cos 2\varphi \rangle \neq 0$ and $\langle \cos 4\varphi \rangle \neq 0$.

In addition to the uniform phases we wish to study the thermodynamic stability of layered mesophases with a density modulation along the macroscopic $Z$-axis. The orientational order, together with the degree of one dimensional (1D) positional order, is used to characterize the layered phases. In close analogy to the uniform phases, there are three distinct orthogonal smectic phases; the uniaxial smectic, $S_U$, with the symmetries of the conventional SmA phase, the tetratic smectic, $S_T$, and the biaxial smectic, $S_{BX}$. The identification of the different uniform or layered phases is based on mean field considerations of molecular symmetry and therefore assumes that the molecular ordering, orientational and/or positional, is of long range.

### A. Two component mixtures

We first consider the theory for a mixture of two species, A and B. To study the liquid crystalline phase transitions we have extended the variational cluster expansion method[26,51] to include not only the orientational ordered phases but also phases with 1D positional order. According to this approach, which is an extension of the Onsager molecular theory for uniaxial nematics,[52] the Helmholtz free energy of the system, $F$, and the distribution functions, $f_i(z,\varphi)$, for the different species ($i$ = A, B) are calculated in terms of the intermolecular potential. To this end the evaluation the following integral is needed

$$q_{ij}(z_{1,2}, \varphi_{1,2}) = \int \mathrm{d}x_{1,2}\ \mathrm{d}y_{1,2}(1 - \exp[-\beta u_{ij}(\boldsymbol{r}_{1,2}, \varphi_{1,2})]). \quad (1)$$

For hard-body intermolecular interactions the function $q_{ij}(z_{1,2}, \varphi_{1,2})$ is simply the area that is excluded to a particle (labelled as particle 1) with dimensions $(a_i, b_i, c_i)$ by a second one (labelled as particle 2) with dimensions $(a_j, b_j, c_j)$ for a relative orientation $\varphi_{1,2}$ and projection, $z_{1,2}$ of the intermolecular vector on the molecular $z$-axis. Straightforward geometrical considerations lead to the following closed form expression for the integral in eqn. (1),

$$\begin{aligned} q_{ij}(z_{1,2}, \varphi_{1,2}) = {} & (b_j c_j + b_i c_i + |\cos \varphi_{1,2}|(c_i b_j + c_j b_i) \\ & + |\sin \varphi_{1,2}|(c_i c_j + b_i b_j)) \\ & \times \Theta\left(\left(\frac{a_i + a_j}{2}\right)^2 - z_{1,2}^2\right) \end{aligned} \quad (2)$$

in which $\Theta$ denotes the step-function; $\Theta(x) = 1$ or 0 for $x \geq 0$ or $x < 0$, respectively.

For a binary mixture with number density $\rho = N/V$ and compositions $x_A$ and $x_B = (1 - x_A)$, the single particle distribution functions for the two components are given by

$$\begin{aligned} f_i(z_1, \varphi_1) &= \frac{1}{\zeta_i} \exp\Big[-\rho d\Big(x_i \langle q_{ii}(z_{1,2}, \varphi_{1,2})\rangle_{f_i(z_2,\varphi_2)} \\ &\qquad + x_j \langle q_{ij}(z_{1,2}, \varphi_{1,2})\rangle_{f_j(z_2,\varphi_2)}\Big)\Big] \\ &= \frac{1}{\zeta_i} \exp[-\rho d \bar{q}_i(z_1, \varphi_1)]. \end{aligned} \quad (3)$$

with $\zeta_i$ the normalisation constant,

$$\zeta_i = \int_0^d \mathrm{d}z \int_0^{2\pi} \mathrm{d}\varphi \exp[-\rho d \bar{q}_i(z,\varphi)]. \tag{4}$$

In these equations $d$ is the layer spacing of the smectic phase such, that $f_i(z \pm nd, \varphi) = f_i(z,\varphi)$, with $n = 1,2,\ldots$ and the subscripts of the angular brackets indicate the distribution functions with respect to which the averaging is taken. In more elaborate calculations, $\rho$ is replaced by an effective density[51,53,54] but this would constitute an unnecessary complication in view of the other simplifications introduced in the present model.

To determine the single particle distribution functions $f_i$ for given $\rho$ and $x_i$ (eqn. (3)) are solved iteratively. For each of the phases studied, the iterative procedure is initiated with trial distribution functions of the appropriate symmetry. Having obtained all the possible solutions for the given thermodynamic conditions and for values of the layer spacing in the range $1/2 \min\{\{a_A, a_B\} \leq d \leq 3 \max\{a_A, a_B\}$, the thermodynamically stable phase is identified as the solution that yields the lowest value for the free energy density of the system. The latter is evaluated from the expression

$$\begin{aligned}\frac{\beta F}{N} &= \ln \rho - 1 + \sum_i x_i \ln x_i - \sum_i x_i \ln \zeta_i/d \\ &\quad - \frac{1}{2}\rho d \sum_{ij} x_i x_j \langle q_{ij}(z_{1,2}, \varphi_{1,2}) \rangle_{f_i,f_j},\end{aligned} \tag{5}$$

where the summation indices run over the molecular species A and B. All the transitions between the phases studied are of second order. To ensure that these phases correspond indeed to the global minimum of the free energy and, therefore, that the system does not separate into two coexisting phases, I and II, with different densities and compositions, we check for possible solutions of the following three coexistence equations

$$\begin{aligned}P^{\mathrm{I}}(x_{\mathrm{A}}^{\mathrm{I}}, \rho^{\mathrm{I}}) &= P^{\mathrm{II}}(x_{\mathrm{A}}^{\mathrm{II}}, \rho^{\mathrm{II}}) \\ \mu_i^{\mathrm{I}}(x_{\mathrm{A}}^{\mathrm{I}}, \rho^{\mathrm{I}}) &= \mu_i^{\mathrm{II}}(x_{\mathrm{A}}^{\mathrm{II}}, \rho^{\mathrm{II}}),\end{aligned} \tag{6}$$

using the molar fraction of the component A in phase I as a free parameter. In eqn. (6), $P^{\mathrm{I}}$ ($P^{\mathrm{II}}$) is the pressure of phase I (II) and $\mu_i^{\mathrm{I}}$ ($\mu_i^{\mathrm{II}}$) is the chemical potential of species $i$ = A, B in phase I (II). No phase coexistence is detected for any of the systems studied, in accord with the second order character of the phase transitions.

### B. Single component systems

Reduction of eqns. (1)–(5) to a single component system yields a straightforward description for the pure phases. In this case, the excluded area function becomes

$$\begin{aligned}q(z_{1,2}, \varphi_{1,2}) &= bc\left(2 + 2\,|\cos \varphi_{1,2}\,| + \left(r + \frac{1}{r}\right)|\sin \varphi_{1,2}\,|\right) \\ &\quad \times \Theta\left(a^2 - z_{1,2}^2\right),\end{aligned} \tag{7}$$

where the transverse aspect ration $r = b/c$ is taken as the quantitative measure of the molecular biaxiality. The distribution function has the form

$$f(z_1, \varphi_1) = \frac{1}{\zeta} \exp[-\rho d \bar{q}(z_1, \varphi_1)], \tag{8}$$

with

$$\begin{aligned}\bar{q}(z_1, \varphi_1) = \langle q(z_{1,2}, \varphi_{1,2}) \rangle_f &= \int_{z_1-a}^{z_1+a} \mathrm{d}z_2 \int_0^{2\pi} \mathrm{d}\varphi_2 f(z_2, \varphi_2) \\ &\quad \times q(z_{1,2}, \varphi_{1,2}),\end{aligned} \tag{9}$$

where the limits for the $z_2$ integration are determined by the hard-body character of the function $q(z_{1,2}, \varphi_{1,2})$ which vanishes outside the range $|z_{1,2}| < a$.

We proceed with a stability analysis of the $\mathrm{N_U}$ with respect to the $\mathrm{N_{BX}}$ and to the $\mathrm{S_U}$ phases by assuming that the single particle pseudo-potential $\bar{q}(z,\varphi)$ for the $\mathrm{N_{BX}}$ and the $\mathrm{S_U}$ phases can be written respectively as

$$\bar{q}_{\mathrm{N_{BX}}}(z, \varphi) = C_0 + \tau C_{\mathrm{T}}(\varphi) \tag{10}$$

and

$$\bar{q}_{\mathrm{S_U}}(z, \varphi) = C_0 + \lambda C_\lambda(z) \tag{11}$$

where $C_\tau(\varphi) = \sqrt{1/\pi}\cos(2\varphi)$, $C_\lambda(z) = \sqrt{2/d}\cos(2\pi z/d)$ and $\tau$ and $\lambda$ are expansion parameters that vanish in the uniaxial nematic phase and acquire non-vanishing but small values near the $\mathrm{N_U}$–$\mathrm{N_{BX}}$ and $\mathrm{N_U}$–$\mathrm{S_U}$ phase transitions, respectively. Expanding eqn. (8) with respect to the expansion parameters $\tau$ and $\lambda$, and neglecting quadratic or higher terms, and taking into account that $\tau = \int_0^{2\pi} \mathrm{d}\varphi C_\tau(\varphi) \bar{q}_{\mathrm{N_U}}(z, \varphi)$ and $\lambda = \int_0^d \mathrm{d}z C_\lambda(z) \bar{q}_{\mathrm{S_U}}(z, \varphi)$, we find the following conditions for the phase transitions

$$\rho_{\mathrm{N_U\text{-}N_{BX}}} = \frac{1}{abc}\frac{3\pi}{4}\frac{r}{(1-r)^2} \tag{12}$$

and

$$\rho_{\mathrm{N_U\text{-}S_U}} = -\frac{1}{abc}\frac{2\pi a/d}{\sin(2\pi a/d)}\frac{\pi r/4}{(1+r)^2 + \pi r} \tag{13}$$

The right hand side of eqn. (13) takes its minimum positive value when $d \approx 1.398a$, which gives the layer spacing at the transition. The three phases merge at a triple point when $\rho_{\mathrm{N_U\text{–}NBX}} = \rho_{\mathrm{N_U\text{–}SU}}$. This condition allows the calculation of the critical value of the molecular biaxiality, $r_c \approx 15.297$, which gives the limit for the molecular biaxiality below which the biaxial nematic phase cannot occur. The packing fraction at which the three phases merge is then calculated from eqn. (13) for $r = r_c$ and it is $\rho_c v_0 \approx 0.176$ where $v_0 = abc$ is the molecular volume.

### C. Computer simulations

To test the predictions of the theory, we have performed computer simulations to determine the phase diagram for the single component system and for three different equimolar mixtures. The crucial feature of any hard-body simulation is the overlap routine and, for the case of aligned board-like biaxial particles, this is particularly simple. If the separation of two similar particles resolved along the director is greater than their height, then they cannot overlap. If this separation is less than the height, then the overlap test reduces to a test for overlapping rectangles in a plane, which further reduces to a sequence of overlap tests for line segments in two dimensions.[55,56] For the infinitely thin case (when $c$ is zero), we need perform only a single line segment test. The overlap test for two particles of differing height is also straightforward, with the average of the two heights replacing the height. The single component system was studied using constant pressure simulations for a range of molecular biaxialities $r = b/c$ between four and infinity; for finite values of the aspect ratio, systems of 500 particles were used, whilst for $b/c = \infty$, larger systems of 1000 and 4000 were used. The simulation box was taken to be rectangular, and the dimensions of the box were allowed to change independently of each other. As already noted, as the system is aligned the phase behaviour is independent of the height ($a$) of the particle, which influences the pressure and density only *via* a simple scaling relation; pressure $P^* = P/ab^2$, density $\rho^* = Nab^2/V$, where $N$ is the number of particles. In practice, we chose the height $a = 1$, the width $b = 1$ and breadth

$c = 1/r$ for the simulations. The simulations for the finite aspect ratio systems (500 particles) were started from a simple lattice with either four or five layers of 125 or 100 particle per layer, respectively. The simulations were typically run for 50,000 cycles to equilibrate the system and then a further 250,000 cycles to calculate the properties of the system, although longer runs of up to 500,000 cycles were used in the vicinity of the transitions. Both compression and expansion runs were used.

In addition to the equation of state for each system, we also require two order parameters to identify the phases, one to measure the biaxiality of the system and the other to measure the extent of the layering. We measure the biaxiality through the biaxial order parameter $\langle \cos 2\phi \rangle$. To characterize the layering of the system, we calculate the structure factor along a direction parallel to the director for a range of wave vectors corresponding to a layer spacing of $a/2$ up to $3a$. When the system is layered, the structure factor for the wave vector corresponding to the layer spacing has a value of $O(N)$, whereas this is $O(1)$ for non-layered systems.[57] The height and location of the maximum in the structure factor therefore provides information both on the extent of smectic order and the layer spacing. Typical plots of the orientational and positional order parameters are shown either side and close to the switch over between $\mathrm{N_U}$–$\mathrm{S_U}$–$\mathrm{S_{BX}}$ and $\mathrm{N_U}$–$\mathrm{N_{BX}}$–$\mathrm{S_{BX}}$ behaviour in Fig. 1. Since the transitions in this aligned system are expected to be continuous, it is difficult to pin down the exact densities at which they occur. To be consistent for the different aspect ratios, we take the biaxial ordering transition to occur at the density at which $\langle \cos 2\phi \rangle = 0.5$ and the layering transition to occur at the density at which the height of the peak in the structure factor is 1/5th of its theoretical maximum. Whilst this gives us a reasonable indication of the densities at the transitions, these are clearly approximate as they depend on our criterion for deciding when the transition has occurred. However, over a large proportion of the range of biaxialities studied, the simulations give a good indication of the phase sequence, although the continuous nature of the transitions makes determining the phase sequence difficult near $r \sim 10$ (see Fig. 1(b)).

## III. Phase diagram of monodisperse biaxial rods

The phase diagrams for the single component systems determined by theory and simulation are shown in Fig. 2. The topology of the phase diagrams determined by the different methods is clearly very similar, although we note that the molecular biaxiality $r$ at which the cross over from $\mathrm{N_U}$–$\mathrm{S_U}$ to $\mathrm{N_U}$–$\mathrm{N_{BX}}$ behaviour is slightly higher for the phase diagram obtained by theory compared to that determined by simulation. Since the $\mathrm{N_U}$–$\mathrm{N_{BX}}$ and $\mathrm{N_U}$–$\mathrm{S_U}$ transitions in this aligned system are continuous, it is difficult to pin down the exact transition density from the order parameters determined in the simulation, but we can get a rough idea of the location of the transition and a good idea of the phase sequence. The situation is even worse near the cross over from $\mathrm{N_U}$–$\mathrm{S_U}$ to $\mathrm{N_U}$–$\mathrm{N_{BX}}$ behaviour since both order parameters increase over the same density range and so we cannot be totally sure if we even get the phase sequence correct in the vicinity of the cross over point. We should also point that since the simulations were performed on relatively small systems, both the smectic and biaxial correlations may be enhanced compared to those expected in a larger system due to the small size of the box. Whilst this might shift the transition densities slightly, it is not clear if this would change the phase sequence for a particular molecular biaxiality and thus shift the cross over point. However, even with these possible failings in the simulations, it is clear that the theory and simulation do indeed give a very similar topology for the phase diagram.

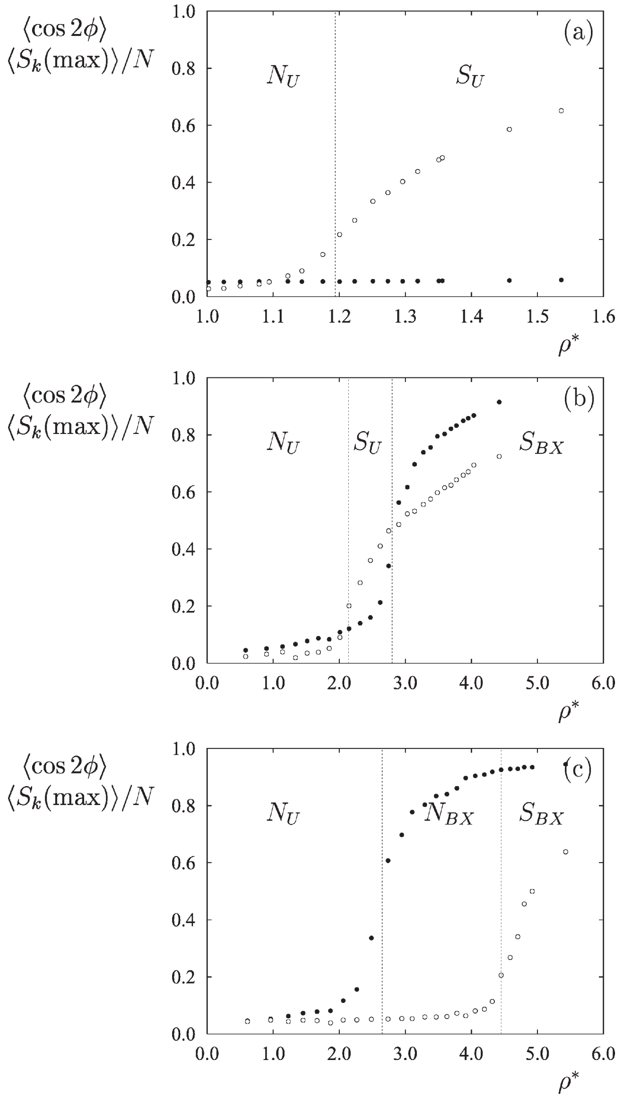

**Fig. 1** Simulation data for (●) the biaxial order parameter $\langle \cos 2\phi \rangle$ and (○) the height of the maximum in the structure factor $\langle S_k(\mathrm{max}) \rangle / N$ as a function of density $\rho^* = Nab^2/V$ for different aspect ratios (a) $r = 4$, (b) $r = 10$ and (c) $r = 15$. The vertical lines indicate the approximate locations of the transitions. For clarity, only compression data is shown.

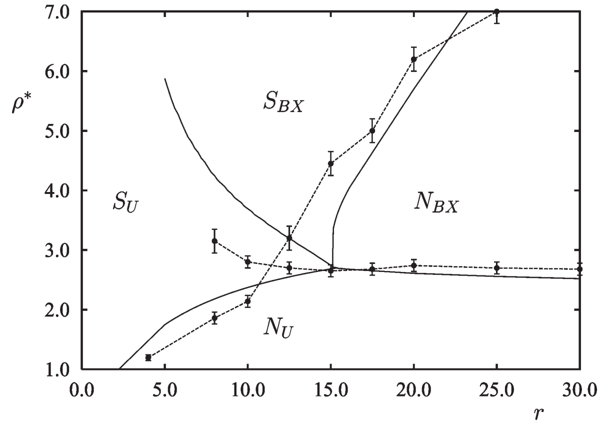

**Fig. 2** The phase diagram for monodisperse hard-body lath-shaped molecules as a function of their molecular biaxiality (transverse aspect ratio $r$); $\rho^* = Nab^2/V$. The circles with the error bars correspond to the simulation results for the transition densities; the dotted line serves as a guide to eye. The solid lines correspond to the theoretical predictions.

Both phase diagrams indicate that the density at which the $N_U$–$N_{BX}$ phase transition takes place is essentially independent of $r$, once this is greater than about 10:1. This phenomenon is similar to that observed for the nematic–isotropic transition for hard disc models, where cut spheres of aspect ratio less than 0.1 behave in essentially the same way as infinitely thin discs.[58] It is also apparent in Fig. 2 that the slope of the $N_{BX}$–$S_{BX}$ line is very sharp near the critical biaxility for both theory and simulations. Furthermore, the agreement between theoretical and simulated phase diagrams improves as the biaxiality $r$ increases and this is consistent with the increasing accuracy of the theory with $r$, becoming the two-dimensional Onsager model[52,59] in the limit of infinite $r$.

We close the discussion of the single component phase diagram by noting that the tetratic nematic and smectic phases, allowed by the theoretical calculations, occurs at fairly low values of $r$ ($r < 1.5$) and higher densities than those shown in Fig. 2. Accordingly it is very likely that this phase is preempted by the formation of a solid and in any case is not relevant to the stability of the biaxial nematic phase.

## IV. Length bidisperse mixtures of biaxial rods

Having successfully tested the reliability of the theoretical predictions using computer simulations, at least for single-component systems and on a semi-quantitative level, we proceed to the theoretical calculations for binary mixtures of lath-shaped rectangular boxes of the same transverse dimensions $b$, $c$ but differing in their length $a$.

We present results for systems of molecular length ratio 0.6. Aside from avoiding length matching, such as lengths in the ratio 1:2, which could possibly favour accidental intra-layer sublayering, the choice of length ratios is somewhat arbitrary. Phase diagrams are presented in Fig. 3 for three binary mixtures differing in the (common) molecular biaxiality $r$ of the two components. The biaxialities chosen are $r = 8$, 10 and 17.5. Since the first two values yield a phase sequence $N_U$–$S_U$–$S_{BX}$ for the monodisperse system, they are suitable for testing the extent to which length bidispersity could enhance the relative stability of the biaxial nematic phase. In contrast, the monodisperse system for $r = 17.5$ exhibits a $N_U$–$N_{BX}$–$S_{BX}$ phase sequence and so we can investigate whether the range over which the biaxial nematic phase is stable can be extended by introducing length dispersity.

It is clear from Fig. 3(a) and (b) that for both $r = 8$ and 10, a stable biaxial nematic can be observed in a binary mixture. For $r = 8$ a small $N_{BX}$ window appears at low concentrations of the long component. The biaxial window for the system with $r = 10$ is quite large and extends over a much larger range of molar fractions from $x_A = 0.15$ to 0.65. An important outcome of both phase diagrams is that the 50:50 mixture is not the optimal mixture for the biaxial nematic phase. Whilst a $N_{BX}$ phase is observed for the 50:50 binary mixture with $r = 10$, the range is relatively small in comparison to the 30:70 mixture; for the system with $r = 8$, a $N_{BX}$ phase is not found for the 50:50 mixture but is present over a narrow range for mixtures in which the concentration of the longer species is lower. Another noteworthy feature of the phase diagrams in Fig. 3(a) and (b) is that the concentration bounds of the biaxial nematic are four-phase merging points; that is, $N_U$, $N_{BX}$, $S_U$ and $S_{BX}$ phases all merge at these points on the ($\eta^*$,$x$) diagram. For the case $r = 17.5$ (Fig. 3(c)), where the phase sequence $N_U$–$N_{BX}$–$S_{BX}$ is observed for a monodisperse system, we observe that the range of the biaxial nematic phase is greatly enhanced for the mixture compared to the monodisperse system. We again observe that the optimal mixture is not centred at 50:50, but shifted to lower values for the concentration of the longer species. All the mixtures in Fig. 3 are stable against demixing in all the phases considered. This stability is a consequence of choosing the components of the bidisperse mixtures to have identical cross-sections and is further enhanced by the alignment of the bidisperse molecular direction along a common director.[60]

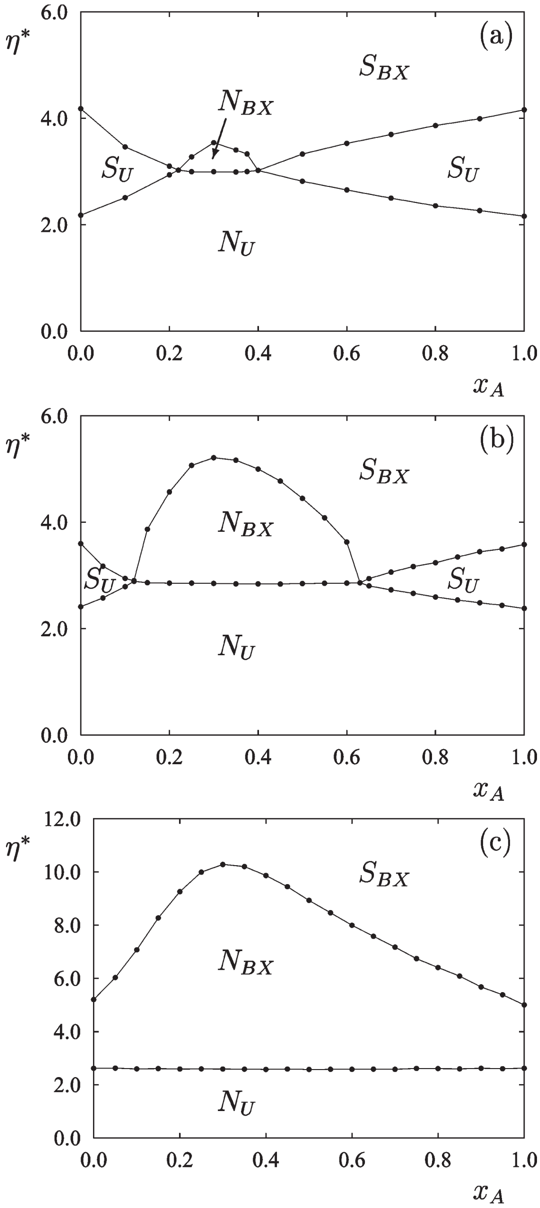

**Fig. 3** Theoretical phase diagrams for length bidisperse mixtures with molecular length ratio $a_B/a_A = 0.6$; reduced density, $\eta^* = (N/V)b^2(a_A x_A + a_B x_B)$ against concentration of the long component, $x_A$. Both components, A and B, have the same biaxility $r$: (a) $r = 8$, (b) $r = 10$ and (c) $r = 17.5$.

## V. Discussion and conclusions

We have shown that systems of aligned biaxial lath shaped particles exhibit a phase sequence that depends on their cross sectional aspect ratio, which is identified as the 'molecular biaxiality'. Single component systems of particles with a large molecular biaxiality exhibit a uniaxial nematic phase, followed by a biaxial nematic and a biaxial smectic phase on increasing the density. The density range over which the biaxial nematic phase is observed is gradually reduced as the cross sectional aspect ratio is lowered. Eventually, the biaxial nematic phase is no longer observed, rather the uniaxial nematic phase undergoes a transition to a unixial smectic, which is then followed by a biaxial smectic phase. The major result of this work is that the cross over point, at which the biaxial nematic phase is stabilized with respect to the uniaxial smectic phase, can be shifted to lower aspect ratios by using mixtures in which the particles have identical cross section dimensions but differ in their lengths. The use of such mixtures may possibly lead to the observation of biaxial nematic phases for molecules having less extreme molecular biaxialities than would be required for single component systems. The model systems chosen to illustrate this possibility, as well as the statistical mechanics analysis used, are of course too simplified to offer any quantitatively usable information for molecular design purposes. However, this work has shown that the basic principle of destabilising the competing smectic phases by using mixtures of lengths does indeed lead to the increased stability of the biaxial nematic phase. The results also indicate that 50:50 mixtures are not optimal for the observation of the biaxial nematic phase.

We can compare the behaviour of this three dimensional (3D) system with that observed in two dimensions (2D). Since our system is perfectly aligned, a cut through the 3D system at constant $z$ leads to a 2D system of hard rectangles of length $b$ and width $c$. Although freely rotating hard rectangles in 2D have not been studied, circular capped rectangles of length $L$ and width $D$ have,[56] and for these no (2D) nematic phase is observed if the aspect ratio $L/D$ is less than about 7; due to the extra circular cap, this apect ratio is similar to rectangles with $b/c = 8$. Thus we would not expect to observe a biaxial nematic phase for hard body, length disperse mixtures when the common cross sectional aspect ratio is less than $b/c \simeq 8$, no matter how disperse the lengths are. This 2D system therefore gives us an approximate lower bound for the cross section at which a biaxial nematic phase can exist for 3D hard body systems. Indeed, this seems to be borne out by the theoretical phase diagrams (see Fig. 3), since the biaxial nematic pocket disappears just below $b/c = 8$. Moreover, we did not observe a $S_U$–$S_{BX}$ transition in the simulations for $r < 8$, although this may just occur at much higher densities than those studied. However, a nematic phase has been observed in a 2D model with (anisotropic) attractive interactions with a less extreme aspect ratio (~4).[61] We may speculate that biaxiality in the attractive forces for the 3D model, which we expect for real molecules, may further reduce this lower bound above which the biaxial nematic phase is possible if the lengths are tailored so as to disrupt the smectic phases.

Comparison of the 3D system with 2D systems also introduces an interesting point concerning the long-range nature of orientational order in biaxial phases. Our hard body, aligned system is probably the simplest system in which a biaxial phase can exist and, as we have seen, the biaxial ordering in 3D can be reduced to the orientational ordering in a 2D system. However, most 2D systems of rod-like particles appear to exhibit a continuous Kosterlitz–Thouless (KT) disclination unbinding type transition between the 2D nematic and isotropic phases (see, for example, ref. 56 and references therein). This implies that the orientational order within the slice through the box at constant $z$ is not truly long range but decays algebraically, although claims for true long-range 2D order have been made for some 2D models.[61] Experimentally, monolayer discotic systems with the disc normal parallel to the substrate have been reported to exhibit in-plane alignment corresponding to 2D biaxial ordering.[62] The theory used here to study the aligned system does not account for KT type transitions and the simulations used are not large enough to be able to distinguish between quasi and true long-range order in the system along the second axis. Indeed, in all simulations of biaxial nematics of freely translating particles,[18,32] the box size has not been large enough to determine the nature of the long-range decay of the orientational correlations for the minor axes. In ref. 32, large (3D) systems of 8192 biaxial Gay–Berne particles are used to investigate the structure of the biaxial nematic phase. Although the systems studied in ref. 32 appear to be biaxial nematic, it is not obvious that the relevant correlation function has decayed to a finite value in the long-range limit for the temperature corresponding to the biaxial nematic phase, thus it is not clear that there is true long-range rather than quasi-long-range biaxial order in this system. Relaxing some of the restrictions of our simple aligned system, such as allowing the particles to rotate about the two shorter axes or changes in particle shape, for example, to a hard ellipsoid, will lead to shape and size dispersity within the cut layer at fixed $z$, leading to a system in which the particles are polydisperse in size and shape. However, we do not expect that polydispersity will stabilise 2D long-range orientational order and so we may wonder if true biaxial nematics can exist. Note that this argument applies to pure systems with a single director or mixtures in which the directors are coincident and not to mixtures (such as rod–disc mixtures) in which the directors are non-coincident.

## Acknowledgements

This work was funded by EU TMR (contract FMRXCT-970121). M. A. B. is grateful to the Royal Society and A. G. V. to the 'Karatheodoris Scientific Research Program, University of Patras' for financial support.

## References

1 Oxford Workshop on Biaxial Nematics, ed. D. Bruce, G. R. Luckhurst and D. J. Photinos, *Special Volume, Mol. Cryst. Liq. Cryst.*, 1998, 323.
2 R. Alben, *J. Chem. Phys.*, 1973, **59**, 4299.
3 R. Alben, *Phys. Rev. Lett.*, 1973, **30**, 778.
4 J. P. Straley, *Phys. Rev. A*, 1974, **10**, 1881.
5 L. J. Yu and A. Saupe, *Phys. Rev. Lett.*, 1980, **45**, 1000.
6 G. R. Luckhurst and S. Romano, *Mol. Phys.*, 1980, **40**, 129.
7 Y. Rabin, W. E. McMullen and W. M. Gelbart, *Mol. Cryst. Liq. Cryst.*, 1982, **89**, 67.
8 A. Stroobants and H. N. W. Lekkerkerker, *J. Phys. Chem.*, 1984, **88**, 3669.
9 R. G. Caflisch, Z. Y. Chen, A. N. Berker and J. M. Deutch, *Phys. Rev. A*, 1984, **30**, 2562.
10 Z. Y. Chen and J. M. Deutch, *J. Chem. Phys.*, 1984, **80**, 2151.
11 D. W. Allender, M. A. Lee and N. Hafiz, *Mol. Cryst. Liq. Cryst.*, 1984, **110**, 331.
12 P. Palffy-Muhoray, J. R. de Bruyn and D. A. Dunmur, *Mol. Cryst. Liq. Cryst.*, 1985, **127**, 301.
13 P. Palffy-Muhoray, J. R. de Bruyn and D. A. Dunmur, *J. Chem. Phys.*, 1985, **82**, 5294.
14 S. R. Sharma, P. Palffy-Muhoray, B. Bergsen and D. A. Dunmur, *Phys. Rev. A*, 1985, **32**, 3752.
15 B. Mulder, *Liq. Cryst.*, 1986, **1**, 539.
16 B. Mulder, *Phys. Rev. A*, 1989, **39**, 360.
17 R. Holyst and A. Poniewierski, *Mol. Phys.*, 1990, **69**, 193.
18 M. P. Allen, *Liq. Cryst.*, 1990, **8**, 499.
19 H. F. Leube and H. Finkelmann, *Makromol. Chem.*, 1991, **192**, 1317.
20 R. Hashim, G. R. Luckhurst, F. Prata and S. Romano, *Liq. Cryst.*, 1993, **15**, 283.
21 R. Van Roij and B. Mulder, *J. Phys. II Fr.*, 1994, **4**, 1763.
22 J. M. Goetz and G. L. Hoatson, *Liq. Cryst.*, 1994, **17**, 31.
23 F. Biscarini, C. Chiccoli, P. Pasini, F. Semeria and C. Zannoni, *Phys. Rev. Lett.*, 1995, **75**, 1803.
24 A. Ferrarini, P. L. Nordio, E. Spolaore and G. R. Luckhurst, *J. Chem. Soc., Faraday Trans.*, 1995, **91**, 3177.
25 P. J. Camp and M. P. Allen, *Physica A*, 1996, **229**, 410.
26 A. G. Vanakaras and D. J. Photinos, *Mol. Cryst. Liq. Cryst.*, 1997, **299**, 65.
27 P. J. Camp and M. P. Allen, *J. Chem. Phys.*, 1997, **106**, 6681.
28 S. Chandrasekhar, G. G. Nair, D. S. S. Rao, S. K. Prasad, K. Praefcke and D. Blunk, *Curr. Sci.*, 1998, **75**, 1042.
29 A. Chrzanowska, *Phys. Rev. E*, 1998, **58**, 3229.
30 A. G. Vanakaras, S. C. McGrother, G. Jackson and D. J. Photinos, *Mol. Cryst. Liq. Cryst.*, 1998, **323**, 199.

31 P. J. Camp, M. P. Allen and A. J. Masters, *J. Chem. Phys.*, 1999, **111**, 9871.
32 R. Berardi and C. Zannoni, *J. Chem. Phys.*, 2000, **113**, 5971.
33 S. Sarman, *Phys. Chem. Chem. Phys.*, 2000, **2**, 3831.
34 D. Sokolowska and J. K. Moscicki, *Phys. Rev. E*, 2000, **62**, 5011.
35 A. G. Vanakaras, A. F. Terzis and D. J. Photinos, *Mol. Cryst. Liq. Cryst.*, 2001, **362**, 67.
36 E. P. Sokolova, I. K. Tokhadze and N. A. Smirnova, *Russ. J. Phys. Chem.*, 2001, **75**, 1319.
37 H. H. Wensink, G. L. Vroege and H. N. W. Lekkerkerker, *J. Chem. Phys.*, 2001, **115**, 7319.
38 K. Praefcke, *Mol. Cryst. Liq. Cryst.*, 2001, **364**, 15.
39 G. R. Luckhurst, *Thin Solid Films*, 2001, **393**, 40.
40 A. Galindo, G. Jackson and D. J. Photinos, *Chem. Phys. Lett.*, 2001, **325**, 631.
41 Y. Martinez-Raton and J. A. Cuesta, *Phys. Rev. Lett.*, 2002, **89**, 185 701.
42 S. Varga, A. Galindo and G. Jackson, *J. Chem. Phys.*, 2002, **117**, 7207.
43 S. Varga, A. Galindo and G. Jackson, *Phys. Rev. E*, 2002, **66**, 11 707.
44 M. C. Artal, K. J. Toyne, J. W. Goodby, J. Barbera and D. J. Photinos, *J. Mater. Chem.*, 2001, **11**, 2801.
45 B. R. Acharya, A. Primak, S. Kumar, T. J. Dingemans and E. T. Samulski, to be published.
46 P. H. J. Kouwer and G. H. Mehl, to be published.
47 R. Pratibha, N. V. Madhusudana and B. K. Sadashiva, *Science*, 2000, **288**, 2184.
48 A. Eremin, S. Diele, G. Pelzl, H. Nadasi, W. Weissflog, J. Salfetnikova and H. Kresse, *Phys. Rev. E*, 2001, **65**, 51 707.
49 A. Stroobants, *Phys. Rev. Lett.*, 1992, **69**, 2338.
50 M. A. Bates and D. Frenkel, *J. Chem. Phys.*, 1998, **109**, 6193.
51 A. G. Vanakaras and D. J. Photinos, *Mol. Phys.*, 1995, **85**, 1089.
52 L. Onsager, *Ann. N. Y. Acad. Sci.*, 1949, **51**, 627.
53 J. D. Parsons, *Phys. Rev. A*, 1979, **19**, 1225.
54 S. D. Lee, *J. Chem. Phys.*, 1987, **87**, 4972.
55 D. Frenkel and R. Eppenga, *Phys. Rev. A*, 1985, **31**, 1776.
56 M. A. Bates and D. Frenkel, *J. Chem. Phys.*, 2000, **112**, 10 034.
57 J. A. C. Veerman and D. Frenkel, *Phys. Rev. A*, 1991, **43**, 4334.
58 M. A. Bates and D. Frenkel, *Phys. Rev. E*, 1998, **57**, 4824.
59 R. F. Kayser and H. J. Raveché, *Phys. Rev. A*, 1978, **17**, 2067.
60 S. DuBois and A. Perera, *J. Chem. Phys.*, 2002, **116**, 6354.
61 J. Tobochnik and G. V. Chester, *Phys. Rev. A*, 1983, **27**, 1221.
62 D. Janietz, *J. Mater. Chem.*, 1998, **8**, 265.